

Mesoscale Numerical Weather Prediction Models Used in Support of Infrared Hyperspectral Measurement Simulation and Product Algorithm Development

JASON A. OTKIN

Cooperative Institute for Meteorological Satellite Studies, University of Wisconsin—Madison, Madison, Wisconsin

DEREK J. POSSELT

Department of Atmospheric Science, Colorado State University, Fort Collins, Colorado

ERIK R. OLSON AND HUNG-LUNG HUANG

Cooperative Institute for Meteorological Satellite Studies, University of Wisconsin—Madison, Madison, Wisconsin

JAMES E. DAVIES

Division of Marine and Atmospheric Research, CSIRO, Hobart, Tasmania, Australia

JUN LI AND CHRISTOPHER S. VELDEN

Cooperative Institute for Meteorological Satellite Studies, University of Wisconsin—Madison, Madison, Wisconsin

(Manuscript received 13 February 2006, in final form 23 June 2006)

ABSTRACT

A novel application of numerical weather prediction (NWP) models within an end-to-end processing system used to demonstrate advanced hyperspectral satellite technologies and instrument concepts is presented. As part of this system, sophisticated NWP models are used to generate simulated atmospheric profile datasets with fine horizontal and vertical resolution. The simulated datasets, which are treated as the “truth” atmosphere, are subsequently passed through a sophisticated forward radiative transfer model to generate simulated top-of-atmosphere (TOA) radiances across a broad spectral region. Atmospheric motion vectors and temperature and water vapor retrievals generated from the TOA radiances are then compared with the original model-simulated atmosphere to demonstrate the potential utility of future hyperspectral wind and retrieval algorithms. Representative examples of TOA radiances, atmospheric motion vectors, and temperature and water vapor retrievals are shown to illustrate the use of the simulated datasets.

Case study results demonstrate that the numerical models are able to realistically simulate mesoscale cloud, temperature, and water vapor structures present in the real atmosphere. Because real hyperspectral radiance measurements with high spatial and temporal resolution are not available for large geographical domains, the simulated TOA radiance datasets are the only viable alternative that can be used to demonstrate the new hyperspectral technologies and capabilities. As such, sophisticated mesoscale models are critically important for the demonstration of the future end-to-end processing system.

1. Introduction

Numerous technological innovations during recent decades have steadily improved our ability to accurately observe the state of the earth’s atmosphere, oceans, and land surfaces from remote sensing plat-

forms. The future development and implementation of progressively more sophisticated infrared imagers and sounders, such as the Advanced Baseline Imager (ABI; Schmit et al. 2005), the Hyperspectral Environmental Suite (HES; Schmit et al. 2003), and the Geosynchronous Imaging Fourier Transform Spectrometer (GIFTS; Smith et al. 2001), will improve the utility of remotely sensed data for weather and climate applications. Efficient data transmission and compression techniques, along with the availability of relatively

Corresponding author address: Mr. Jason Otkin, 1225 W. Dayton St., Madison, WI 53706.
E-mail: jason.otkin@ssec.wisc.edu

cheap storage and powerful computer processors, will provide the capability to fully utilize the immense amount of data that these sensors will produce.

The expected launch of GIFTS during the next decade will usher in a new era of unprecedented capability to image and profile the atmosphere from a geosynchronous orbit. The GIFTS platform will include two large-area-format focal plane detector arrays that will provide near-instantaneous coverage over a large geographical area ($512 \text{ km} \times 512 \text{ km}$) with 4-km horizontal resolution at nadir. A Fourier transform spectrometer will enable the atmospheric radiance spectra for more than 1600 infrared channels (with a spectral resolution of $\sim 0.6 \text{ cm}^{-1}$) to be observed simultaneously for all detector array elements (Smith et al. 2001). The information provided by the vast array of channels will significantly enhance the vertical resolution of temperature and water vapor sounding retrievals to 1–2 km in the troposphere. GIFTS will produce $\sim 80\,000$ soundings per minute, which is expected to have a significant impact on data assimilation. For example, the increased vertical resolution of GIFTS will enhance the usefulness of atmospheric motion vectors for data assimilation by reducing the ambiguity in height-level assignment that currently limits the value of satellite-derived motion vectors. GIFTS will also greatly enhance our ability to monitor severe weather events, characterize surface and cloud microphysical properties, and track the evolution of trace gases in the atmosphere.

The development of GIFTS represents a collaborative effort between the National Aeronautics and Space Administration, the University of Wisconsin—Madison, Utah State University, and the National Oceanic and Atmospheric Administration (NOAA). As part of this joint effort, the Cooperative Institute for Meteorological Satellite Studies (CIMSS) at the University of Wisconsin—Madison is currently developing and testing the GIFTS forward radiative transfer model and retrieval algorithms. Data from existing hyperspectral sensors, such as the Atmospheric Infrared Sounder (AIRS) and the National Polar-Orbiting Operational Environmental Satellite System (NPOESS) Airborne Sounder Test bed Interferometer (NAST-I), have been used to demonstrate the GIFTS retrieval algorithms as well as to empirically estimate the expected accuracy of the GIFTS imaging and sounding products (Smith et al. 2003; Weisz et al. 2003; Li et al. 2004; Wei et al. 2004).

As a complement to these real data sources, an end-to-end processing system that utilizes high-resolution proxy top-of-the-atmosphere (TOA) radiance datasets derived from numerical weather prediction (NWP) model output has been developed. NWP models are critically important within this system because real hy-

perspectral radiance measurements taken with ground-, air-, or space-based systems are not available with fine temporal resolution for large geographical domains. The availability of proxy datasets with temporal and spatial resolution comparable to the anticipated GIFTS sensor configuration supports a realistic demonstration of GIFTS capabilities and measurements. The first step in the end-to-end system is to use a sophisticated NWP model such as the fifth-generation Pennsylvania State University (PSU)—National Center for Atmospheric Research (NCAR) Mesoscale Model (MM5) or the Weather Research and Forecasting (WRF) model to generate realistic high-resolution atmospheric profile datasets for a variety of locations and atmospheric conditions. These datasets, which are treated as the “truth” atmosphere, are subsequently passed through the GIFTS forward radiative transfer model to generate simulated TOA radiances. GIFTS baseline instrument effects, such as random measurement errors, are also included to emulate representative GIFTS radiance measurement characteristics. Atmospheric motion vectors and temperature and water vapor retrievals generated from the TOA radiances are then compared with the original model-simulated atmosphere to demonstrate potential hyperspectral measurement capabilities and the potential utility of future wind and retrieval algorithms.

The primary objective of the numerical modeling work is to produce physically realistic and thermodynamically consistent simulated datasets that contain mesoscale cloud, temperature, and water vapor structures representative of the real atmosphere. The ability to reproduce the exact atmospheric state, however, is constrained by the need to parameterize subgrid-scale processes such as cloud physics, turbulence, and radiation, and by the reduction of the effective model resolution resulting from numerical effects (e.g., see Grasso 2000; Pielke 2002). Aside from these limitations, there are many benefits to using mesoscale models to generate proxy datasets. For instance, the model output frequency and grid spacing can be chosen to match the resolution of the simulated sensor. Another notable benefit is the fact that the simulated datasets are not limited to a specific geographical domain or to a specific time period because the model domain can be chosen for any region of interest for which model initialization data are available. Compared to datasets derived from air- and space-based sensors, it is also very beneficial that the proxy data are available at regular time intervals across the entire geographical domain. Finally, by using proxy datasets, the end-to-end system that will be required to process operational GIFTS data can be fully developed and tested prior to launch since

the data stream within the system is fully transparent and consistent.

In this paper, we document how CIMSS uses meso-scale models, such as the MM5 and WRF, as part of an end-to-end processing system, to demonstrate future hyperspectral measurement capabilities. Although the GIFTS satellite is the primary focus of this paper, the end-to-end system can be easily adapted to other infrared sensors, such as ABI and HES. The forward and mesoscale models are described in detail in section 2. This section also contains an outline of the procedure used to convert the model data and other climatological information (such as ozone) into the format required by the forward model. Results from two case studies will be presented in section 3, with summary comments given in section 4.

2. Model descriptions and methodology

a. Mesoscale models

The MM5 was initially employed for this simulation work. MM5 is a nonhydrostatic numerical model that solves the full nonlinear primitive equations on terrain-following sigma levels. Prognostic variables carried by the model include the perturbation pressure, temperature, vertical and horizontal wind components, and the water vapor mixing ratio. Microphysical quantities, such as the number concentration of ice and the mixing ratios for rainwater, cloud water, ice, snow, and graupel can also be predicted. A 24-category topography and land-use dataset with variable horizontal resolution is used to determine certain surface characteristics, such as albedo, longwave emissivity, roughness length, and heat capacity. A sophisticated land surface model (LSM), developed at the Oregon State University, has been coupled to the MM5 (Chen and Dudhia 2001), and can be used to provide realistic fluxes of heat and moisture at the surface. For a complete description of the MM5 modeling system, the reader is referred to Grell et al. (1994) and Dudhia et al. (2003).

WRF is a sophisticated numerical model that solves the compressible nonhydrostatic Euler equations (cast in flux form) on a mass-based terrain-following coordinate system. The WRF model includes several microphysical, cumulus, and planetary boundary layer (PBL) schemes and also employs the recently developed Noah LSM. High-resolution global datasets are used to initialize the topography and other static surface fields. Prognostic variables include the horizontal and vertical wind components, several microphysical quantities, and the perturbation potential temperature, geopotential, and surface pressure of dry air. WRF employs the third-order Runge–Kutta temporal integration scheme as

well as the sixth-order horizontal and vertical advection schemes. Skamarock et al. (2005) provide a complete description of the WRF model dynamics.

The development of the WRF model represents a major advancement in our ability to realistically simulate mesoscale structures in the atmosphere. The primary reason for this improvement is the adoption of numerical schemes that are more appropriate for the finescale horizontal resolution that we routinely employ for our simulations. Skamarock (2004) showed that the advanced numerics of the WRF model result in an effective resolution of ~ 7 times the horizontal grid spacing, which is a substantial improvement over the MM5. Because our simulated atmospheric datasets are used to produce simulated TOA radiances for a proposed instrument with 4-km horizontal resolution, the ability to effectively resolve small-scale atmospheric structures represents one of the primary advantages to using the WRF model for our simulation work.

b. Forward model

The forward radiative transfer model being developed at CIMSS calculates TOA radiances with very high spectral resolution across the infrared spectrum most likely to be observed by future multi- and hyperspectral sensors. This generic structure maximizes productivity by allowing forward-model development to be applicable to multiple infrared sensors, including ABI, HES, and GIFTS (Tobin et al. 2001; Moy et al. 2004). For GIFTS algorithm development, the high-resolution radiances are spectrally reduced to the GIFTS spectral range. For the case studies discussed in this paper, the forward model employed the Yang et al. (2003) single-layer cloud model, which uses line-by-line radiative transfer code and the discrete ordinate radiative transfer (DISORT; Stamnes et al. 1988) method to parameterize liquid and ice cloud optical properties into transmittance and reflectance functions with high spectral resolution. Because this version of the cloud model can only accommodate a single cloud layer consisting entirely of ice crystals or liquid water droplets, a selection rule must be applied in the presence of mixed-phase or multilevel clouds. For simplicity, the highest altitude cloud phase in a given column is assumed to represent the phase of the cloud to be ingested into the forward model. Although some cloud information will be lost, this approximation is reasonable because the primary source of infrared radiation in a cloudy sky is at or near the cloud top. The reader is referred to Davies et al. (2003) for a more detailed description of the GIFTS forward model. Niu et al. (2007) document the implementation of a new two-layer cloud model, which

will allow for a more realistic treatment of multilayer clouds by the forward model.

c. Forward-model interface

Numerical model output from the MM5 and WRF serves as the main component of the simulated atmospheric datasets ingested by the forward radiative transfer model. Simulated fields used by the forward model include the surface temperature, the atmospheric temperature, and the mixing ratios for water vapor, cloud water, rainwater, ice, snow, and graupel. Effective particle diameters are calculated for each microphysical species using a method adopted from Mitchell (2002), which utilizes the mixing ratio and the number concentration of a given species. An inverse-exponential particle size distribution, along with the microphysical parameters and assumptions explicit to a given microphysics scheme, is used to estimate the number concentrations. Total liquid (cloud water and rainwater) and total ice (ice, snow, and graupel) water paths are calculated using the appropriate microphysical mixing ratios. Liquid and ice cloud-top pressures are identified by searching downward from the model top until a minimum mixing ratio threshold is exceeded in a given grid cell.

Logarithmic interpolation is used to transfer the simulated three-dimensional data from the model's sigma coordinate system to the isobaric coordinate system used by the forward model, which contains 101 unevenly spaced levels extending from 1100 to 0.005 hPa. Temperature and water vapor data on the lowest sigma level is extrapolated downward to fill all forward-model pressure levels located beneath the model topography. Temperature profiles from the National Environmental Satellite, Data, and Information Service (NESDIS) 1200 dataset are used to fill the pressure levels located above the model top (which is generally set to 10 hPa), while the water vapor mixing ratio above this level is set to a value representative of dry stratospheric air. Ozone data extracted from five different model atmospheres in the line-by-line radiative transfer model (LBLRTM; Clough and Iacono 1995) were used to create representative ozone profiles for each grid point in a given dataset.

3. Case studies

In support of GIFTS forward-model and retrieval algorithm development, high-resolution numerical model simulations were performed for several case studies characterized by different atmospheric conditions. In this section, we will examine results from two case studies, including a convective initiation event that occurred

over the Southern Great Plains (SGP) and an extratropical cyclone that developed over the western Atlantic. Validation of the forward model and retrieval algorithms is beyond the scope of this paper; therefore, representative images are only shown to illustrate the use of the simulated datasets and the potential capability of the GIFTS instrument.

a. IHOP convective initiation event

Our first simulated atmospheric profile dataset was generated for a convective initiation event that occurred on 12 June 2002 during the International H₂O Project (IHOP). This event was characterized by the development of an intense line of thunderstorms during the late afternoon and evening hours along a distinct lower-tropospheric dryline that extended from the Texas Panhandle northeastward into southern Kansas (Fig. 1). Low-level wind shear along the dryline was enhanced by the presence of a weak mesoscale cyclonic circulation over northwestern Oklahoma. The atmosphere ahead of the dryline was characterized by strong potential instability with surface temperatures in excess of 30°C and convective available potential energy greater than 2000 J kg⁻¹ (not shown). These conditions produced a favorable environment for convective development.

Version 3.5 of the MM5 was used to produce a realistic simulation of this event. The simulation was initialized at 0600 UTC 12 June 2002 with 20-km rapid update cycle (RUC) data and then run for 24 h on a single 280 × 400 gridpoint domain with 4-km horizontal grid spacing (Fig. 2) and 60 vertical levels. Soil moisture and temperature data used to initialize the MM5 were obtained from 1° Global Data Assimilation System (GDAS) analyses. Abnormally dry hydrological conditions were present across the eastern portion of the domain during this time period; therefore, the climatological vegetation fraction data used by MM5 were replaced by a more realistic estimate derived from the Advanced Very High Resolution Radiometer (AVHRR) Normalized Difference Vegetation Index (NDVI). To better simulate the timing and location of the convective initiation event, the MM5 simulation was nudged toward the RUC analyses during a 6-h spinup period using the MM5 four-dimensional data assimilation (FDDA) system (Stauffer and Seaman 1990). The FDDA nudging coefficients were gradually reduced to zero during the subsequent 1-h period in order to allow the model to smoothly transition from a forced to a freely evolving state. Subgrid-scale processes were parameterized using the Goddard mixed-phase cloud microphysics scheme (Lin et al. 1983; Tao and Simpson 1993a,b), the Medium-Range

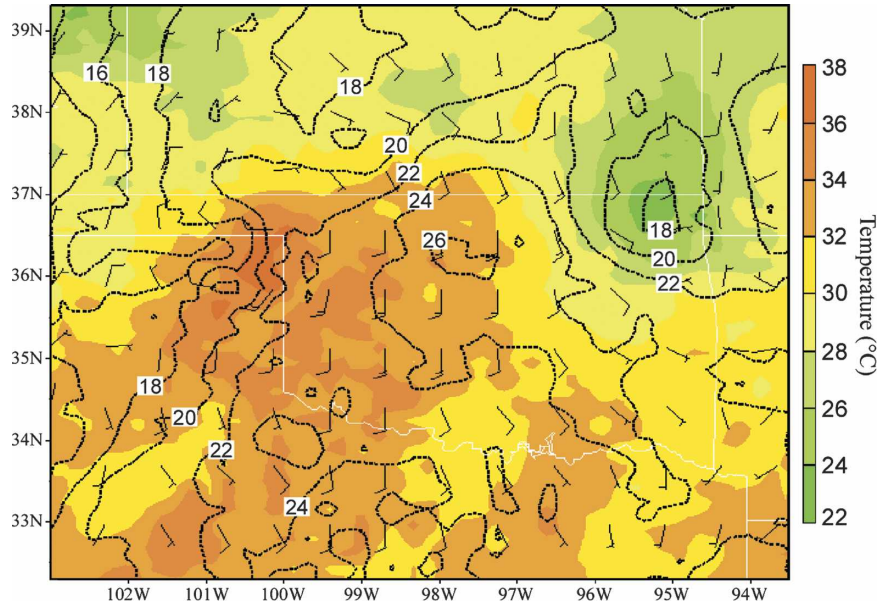


FIG. 1. RUC analyses of 2-m temperature ($^{\circ}\text{C}$; color fill), 2-m dewpoint temperature ($^{\circ}\text{C}$; dashed lines), and 10-m wind vectors (kt) valid at 1800 UTC 12 Jun 2002.

Forecast (MRF) PBL scheme (Hong and Pan 1996), and the Dudhia (1989) shortwave and Rapid Radiative Transfer Model (RRTM) longwave radiation (Mlawer et al. 1997) schemes. No cumulus parameterization scheme was used during the simulation because the horizontal grid spacing was <5 km. The lack of a cumulus scheme results in a more realistic simulation of the cloud structure because only explicitly resolved convection can occur.

The primary objective of this case study was to generate a simulated atmospheric profile dataset that realistically portrayed the evolution of finescale water vapor gradients in clear air prior to convective initiation and the three-dimensional structure of the subsequent deep convection. To assess the ability of the MM5 to

realistically simulate these features, a brief comparison between the observed and model-simulated data is presented here.

Figure 3 compares the evolution of the $10.7\text{-}\mu\text{m}$ infrared brightness temperatures observed by the *Geostationary Operational Environmental Satellite (GOES)-II* with those simulated by the MM5 during a portion of the convective initiation event. Model-simulated brightness temperatures were obtained by converting radiances within the RRTM longwave radiation scheme to brightness temperatures, and then averaging over the GOES $10.7\text{-}\mu\text{m}$ spectral range. Because the MM5 radiances are not explicitly convolved with the GOES weighting function, the comparison is not exact, but it does serve to illustrate the location of lower- and upper-level clouds as well as gradients in near-surface temperature. Figure 3 shows that the MM5 simulation depicted the location and timing of the convective initiation over the Texas Panhandle and western Oklahoma reasonably well. Scattered low-level cloud cover across portions of Kansas and clear-sky conditions over southwestern Oklahoma are also realistically portrayed. An erroneous convective complex over the eastern portion of the MM5 domain (Figs. 3b,d) persisted on the northern side of a well-defined outflow boundary several hours longer than actually observed (the western edge of the real cloud shield is evident in Fig. 3a). Although this feature represents a significant departure from reality, it is relatively unimportant for our work because we are primarily inter-

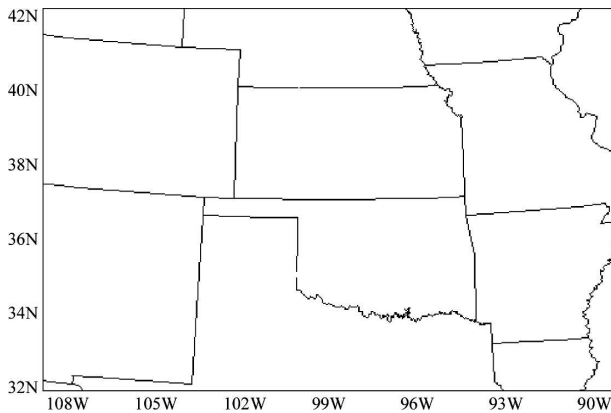


FIG. 2. Geographical domain covered by the MM5 simulation.

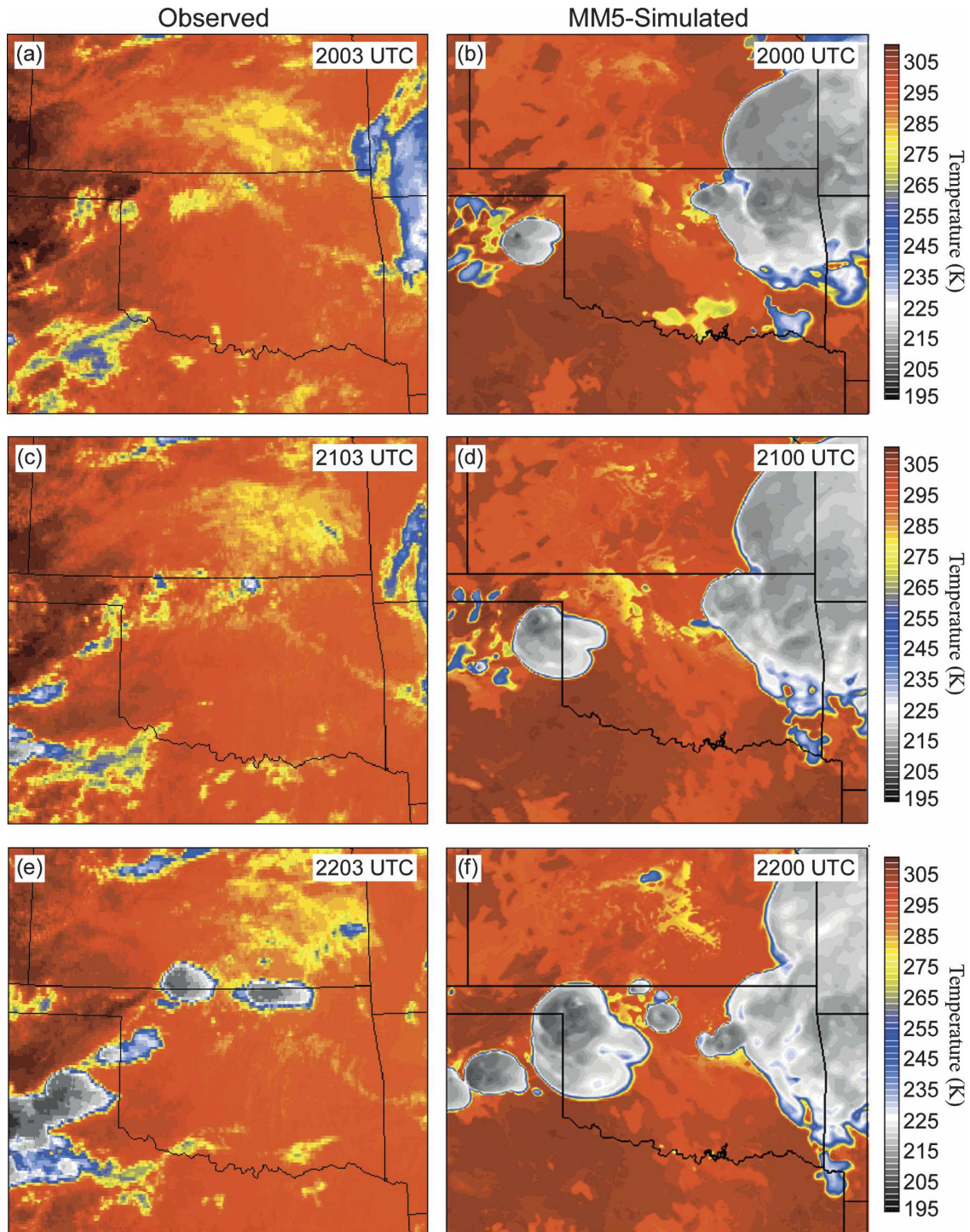


FIG. 3. *GOES-11* 10.7- μm brightness temperatures (K) valid at (a) 2003, (c) 2103, and (e) 2203 UTC 12 Jun 2002. MM5-simulated 10.7- μm brightness temperatures (K) valid at (b) 2000, (d) 2100, and (f) 2200 UTC 12 Jun 2002.

ested in the region surrounding the convective initiation over the western portion of the domain.

Figure 4 shows the evolution of the MM5-simulated low-level wind and moisture fields and the three-

dimensional cloud structure during the early stages of thunderstorm development. At 1900 UTC (Fig. 4a), a weak cyclonic circulation and a tight low-level water vapor gradient were present across the Texas Pan-

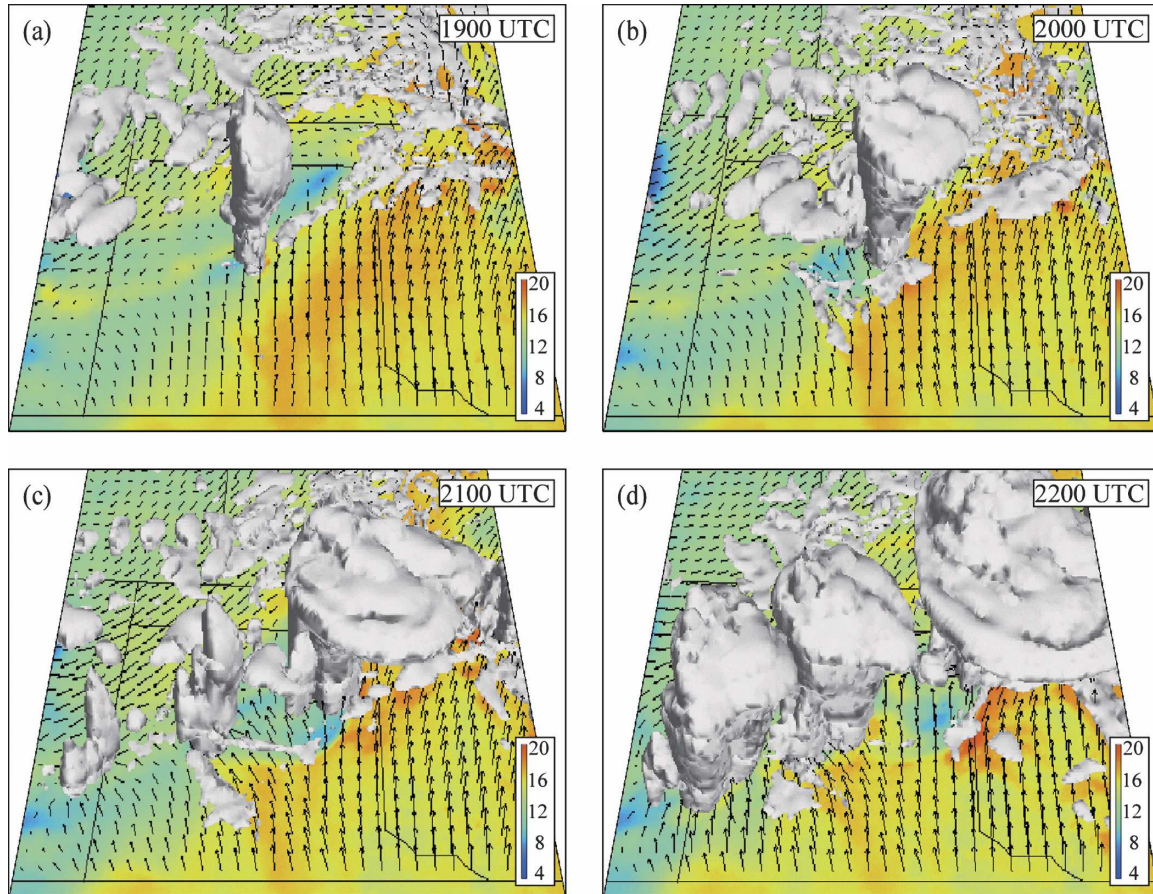


FIG. 4. Simulated three-dimensional cloud structure (total cloud water, rainwater, ice, snow, and graupel mixing ratio greater than 0.1 g kg^{-1} shown in white isosurfaces), 2-m water vapor mixing ratio (g kg^{-1} ; shown in colored horizontal field), and 1.5-km wind vectors valid at (a) 1900, (b) 2000, (c) 2100, and (d) 2200 UTC 12 Jun 2002.

handle. Deep convection subsequently developed across the region with an orientation and horizontal extent comparable to observations (refer to Fig. 3). Qualitative analysis demonstrates that the MM5 simulation contains a realistic depiction of the three-dimensional evolution of the thunderstorms and their surrounding environment. For instance, the initial convective column in Fig. 4a developed into a mature thunderstorm (Fig. 4c) characterized by a large upper-level anvil and a well-defined surface outflow boundary.

Temperature and relative humidity profiles taken as part of the Balloon-Borne Sounding System at four sites in the SGP Atmospheric Radiation Measurement (ARM) network are compared to collocated MM5-simulated profiles in Fig. 5. For this comparison, it is important to note that the observed profiles contain much greater vertical resolution ($\sim 10 \text{ m}$ through the troposphere and lower stratosphere) than the MM5 profiles ($50\text{--}200 \text{ m}$ in the boundary layer and $>200 \text{ m}$ in the free atmosphere). Considering the difference in

vertical resolution, it is not surprising that the MM5 profiles contain less finescale vertical structure than the observed profiles. Many of the structures evident in the observed relative humidity profiles occur over very thin layers ($<200 \text{ m}$) that are simply not resolvable in the MM5 simulation. Although the lack of these very fine-scale structures diminishes the realism of the simulated profiles, it is clear that these profiles still contain a substantial amount of vertical variability; therefore, we maintain that the simulated profiles contain sufficient vertical structure to adequately represent the real atmosphere for our work.

A simulated atmospheric profile dataset was generated for this case using the procedure outlined in section 2. This dataset was subsequently ingested into the GIFTS forward model to generate simulated TOA radiances and brightness temperatures for discrete wavelengths within the GIFTS spectral range. Figure 6 shows representative examples of simulated brightness temperatures during the early stages of thunderstorm

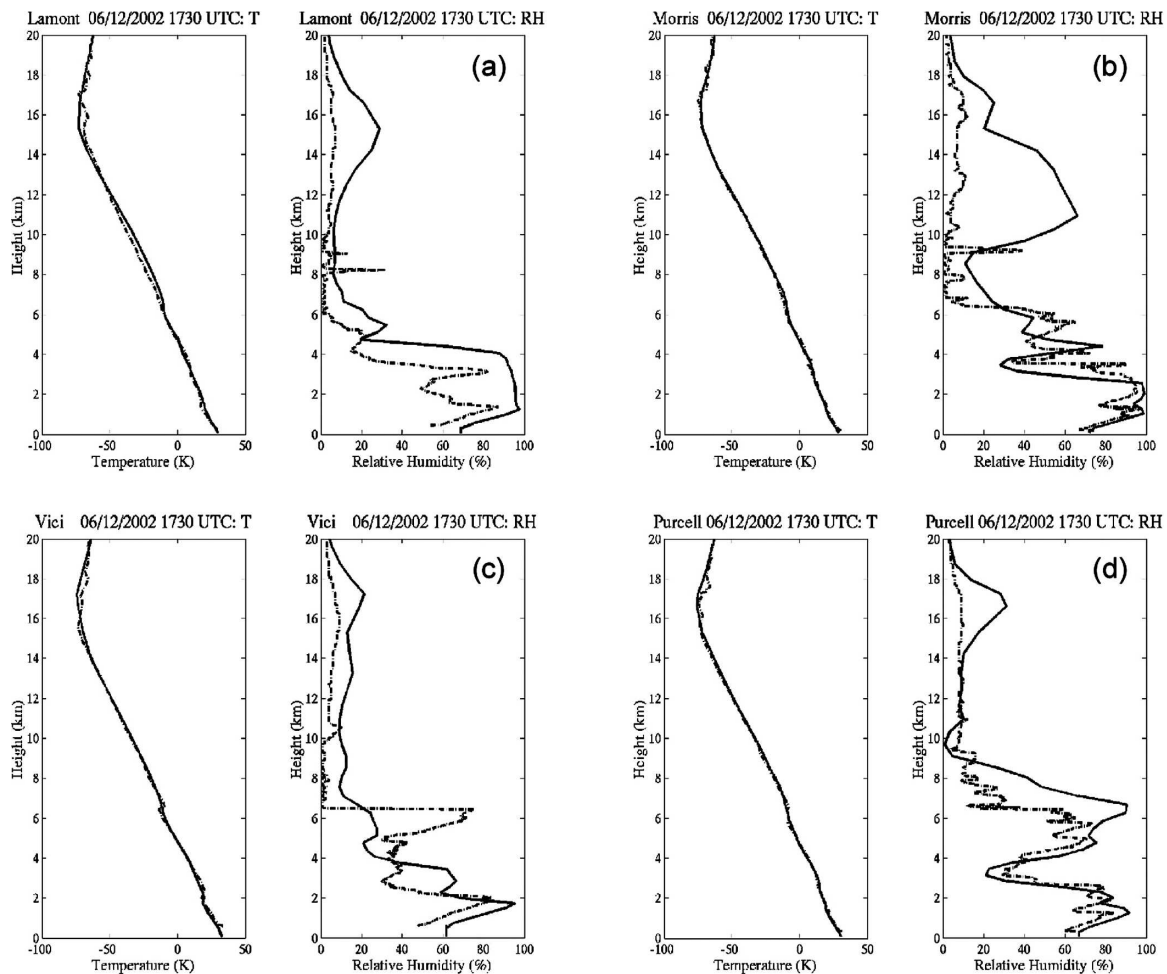


FIG. 5. Observed (dashed line) and MM5-simulated (solid line) temperature and relative humidity profiles valid at 1730 UTC 12 Jun 2002 for four Oklahoma ARM sites: (a) Lamont, (b) Morris, (c) Vici, and (d) Purcell.

development over the Texas Panhandle. Each successive wavelength in Fig. 6 is characterized by a weighting function that is most sensitive to atmospheric emission at a progressively higher altitude (not shown); therefore, the corresponding brightness temperatures can be used to evaluate the aerial extent of cloud cover at different levels in the atmosphere. For instance, the $12.2\text{-}\mu\text{m}$ “window” channel (Fig. 6a) is relatively insensitive to atmospheric gases and can, therefore, be used to identify clouds at all levels in the atmosphere and to view the surface during cloud-free conditions. With this channel, the low-level cloud cover over western Kansas and the upper-level cloud cover associated with the incipient squall line over the Texas Panhandle and the thunderstorm complex over the eastern portion of the domain are both clearly visible. The $5.32\text{-}\mu\text{m}$ channel (Fig. 6b) is sensitive to water vapor emission in the lower atmosphere and is thus unable to detect most of the low-level clouds in western Kansas. Because the

5.67- and $5.64\text{-}\mu\text{m}$ channels (Figs. 6c,d) are characterized by substantially greater water vapor absorption in the lower atmosphere, only the highest and coldest cloud layers associated with the thunderstorm complexes are evident in these images.

TOA radiances generated by the forward model were used by a complex inverse retrieval algorithm (Li et al. 2000; Li and Huang 1999) to generate atmospheric temperature and water vapor profiles. Infrared sensors such as GIFTS are unable to see through thick clouds; therefore, profiles extending down to the earth’s surface are only available during clear-sky conditions. Smith et al. (2004) have recently implemented a new retrieval algorithm that is able to retrieve temperature and water vapor profiles in clear air above the cloud top during cloudy-sky conditions. The extension of the retrieval algorithm to cloudy regions greatly enhances the geographical coverage of the infrared sounding retrievals, especially at higher altitudes, including within and

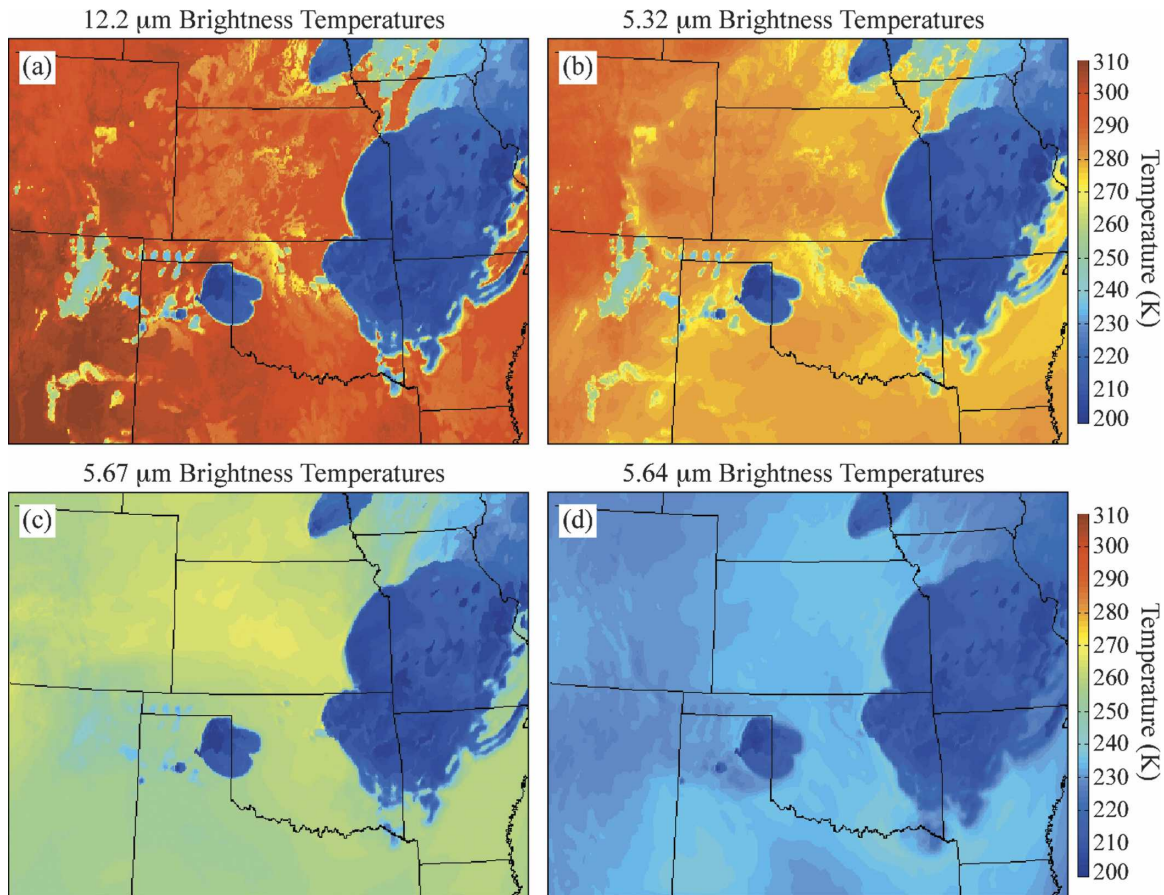


FIG. 6. Simulated brightness temperatures from the GIFTS forward model for the (a) 12.2-, (b) 5.32-, (c) 5.67-, and (d) 5.64- μm infrared channels. All images valid at 2100 UTC 12 Jun 2002.

below thin cirrus clouds. For our work, a cloud mask based on the MM5-simulated cloud-top pressure is applied to the simulated data before the retrievals are performed. Temperature and water vapor data from the MM5 simulation are used as the truth atmosphere to validate the retrieval algorithm performance. Uncertainties in the retrieved products can be objectively quantified through a systematic comparison between the model “truth” and the retrievals. This end-to-end control process is the only viable method to validate every component of the processing system before GIFTS becomes operational. Because a quantitative evaluation of the retrieval algorithm is beyond the scope of this paper, a thorough evaluation of its accuracy will be left to subsequent studies related to algorithm development and validation. To demonstrate one use of the simulated datasets within the end-to-end processing system, Fig. 7 shows a representative comparison of the 850-hPa temperature and water vapor mixing ratio from the MM5 simulation and the GIFTS retrievals. Overall, it is apparent that the temperature fields

are qualitatively similar, while slightly larger differences exist between the moisture fields. It is also evident that the simulated and retrieved data contain mesoscale variability representative of the real atmosphere.

The simulated water vapor retrievals were subsequently used to demonstrate a new atmospheric motion vector (AMV) tracking methodology that operates on isobaric moisture fields derived from hyperspectral soundings. With this approach, the full vertical resolution of the hyperspectral data is used during the retrieval process, with moisture values output on specified pressure levels. A modified version of the CIMSS automated tracking algorithm (Velden et al. 1997) was then applied to a time sequence of images derived from the moisture analyses in order to generate moisture-tracked “winds” within cloud-free regions. The novelty of this approach is that it eliminates much of the uncertainty in traditional AMV height assignment, which is often the largest source of error in satellite-derived winds (Nieman et al. 1993). Figure 8 shows the tracking

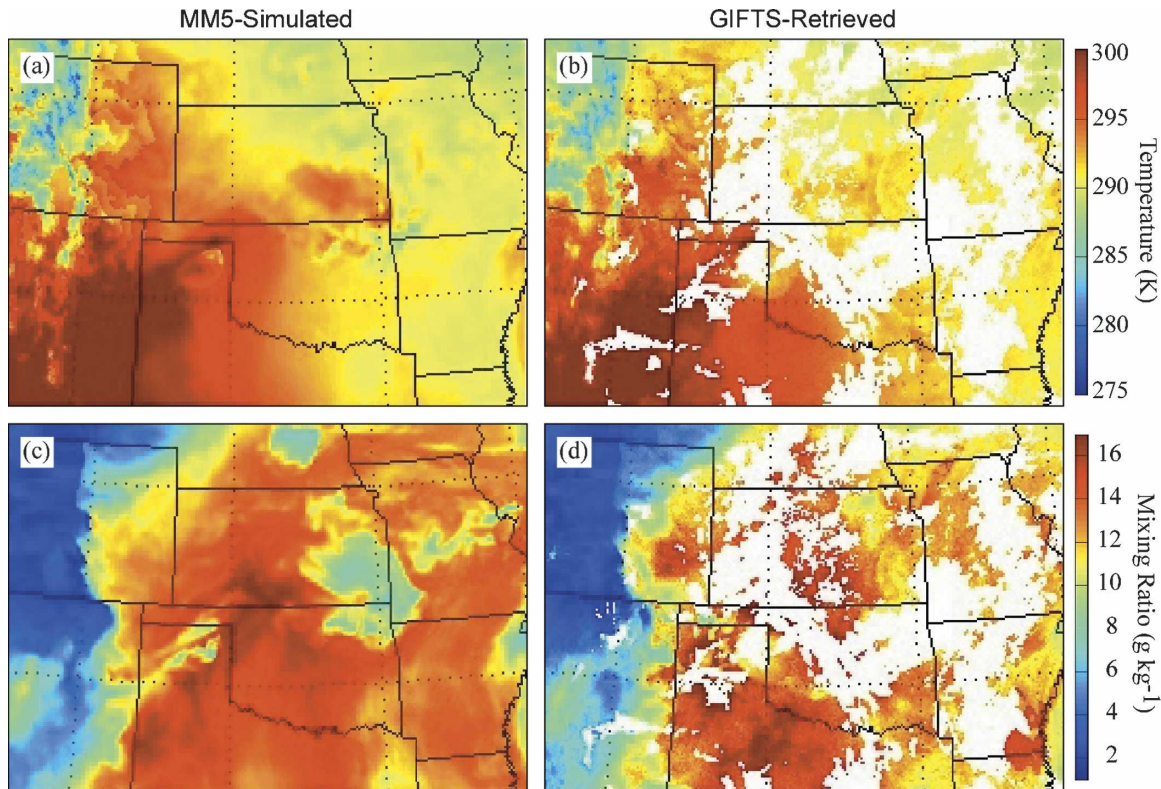


FIG. 7 (a) MM5-simulated and (b) GIFTS-retrieved 850-hPa temperatures (K). (c) MM5-simulated and (d) GIFTS-retrieved 850-hPa water vapor mixing ratio (g kg^{-1}). White areas in the GIFTS-retrieved fields correspond to cloudy regions at or above the 850-hPa level in the MM5 simulation.

results for three experiments designed to represent the lower (“noisy”) and upper (“noiseless”) accuracy bounds expected to occur during standard (“noise filtered”) retrieval conditions. Comparison with the truth AMVs derived directly from the MM5-simulated water vapor mixing ratio field (Fig. 8a) demonstrates that the new concept is achievable, although optimization of the methodology and a thorough evaluation of the wind vector quality are still necessary. For additional information, the reader is referred to Velden et al. (2005).

b. Extratropical cyclone simulation

One goal of the simulation work is to steadily improve our ability to generate high-quality simulated datasets containing realistic atmospheric structures at progressively finer scales. This goal can be achieved in part by employing a numerical model, such as WRF, that is characterized by enhanced effective resolution and is thus better able to simulate finescale atmospheric features. An alternative method is to increase the horizontal and vertical grid spacing of the model simulation. High-resolution simulations covering a large geographical domain, however, require a vast amount of

computer memory and a sufficient number of processors to run in an efficient manner. To perform such large model simulations, a 64-bit Silicon Graphics Inc. (SGI) Altix with 32 processors and 192 Gb of memory was employed. The fast processors and extensive memory resources of the Altix permit the generation of massive high-resolution model simulations in a reasonable amount of time.

As a first step in utilizing these resources, a simulated atmospheric profile dataset was generated for a strong extratropical cyclone that developed along the east coast of the United States during the Atlantic THORPEX (The Observing System Research and Predictability Experiment) Regional Experiment. This cyclone was characterized by an extensive cloud shield that extended from the mid-Atlantic states eastward into the Atlantic Ocean (refer to Fig. 12a). Version 2.0.3 of the WRF model was used to produce a realistic simulation of this event. The simulation was initialized at 0000 UTC 5 December 2003 with 1° Global Forecasting System (GFS) analyses, and then run for 24 h on a single 1070×1070 gridpoint domain (Fig. 9) with 2-km horizontal grid spacing and 50 vertical levels. The simulation employed the WRF single-moment six-class micro-

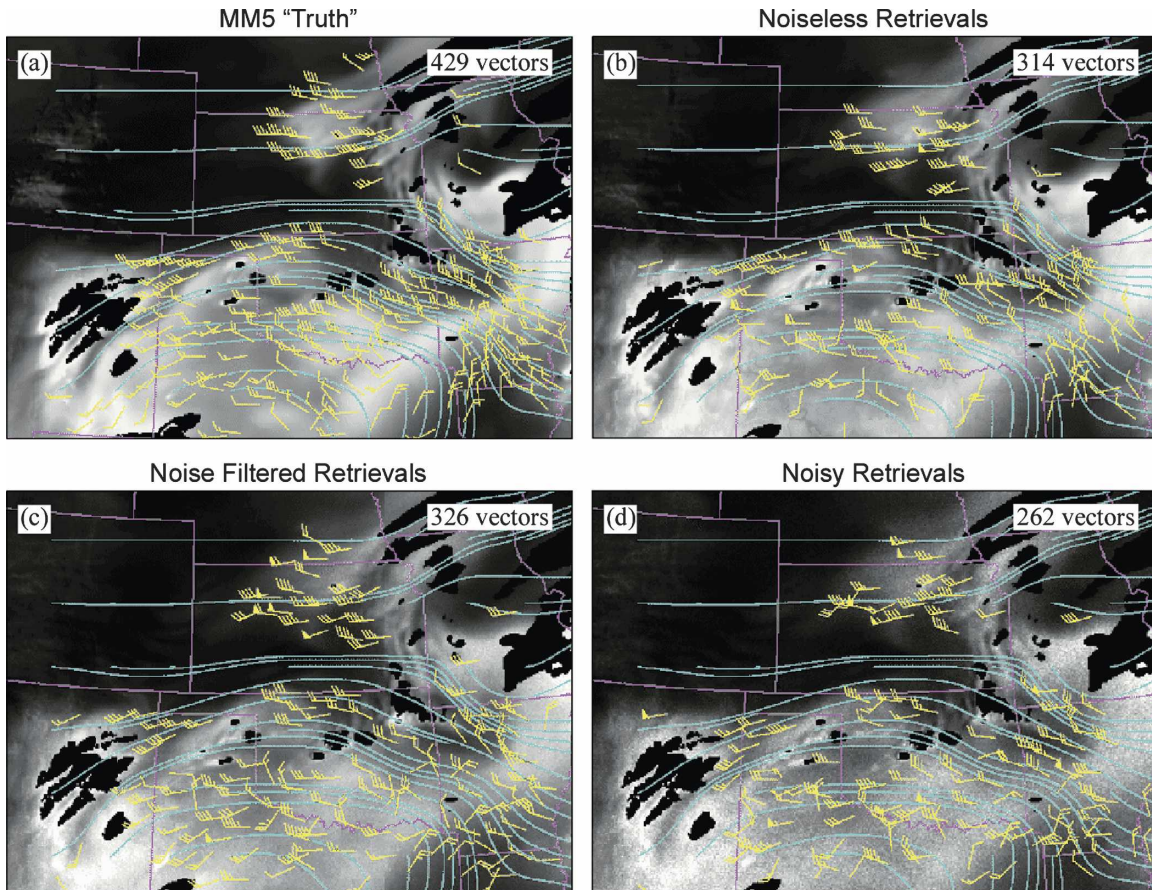


FIG. 8. Simulated 500-hPa wind vectors obtained by tracking three sequential moisture images derived from (a) MM5 water vapor analyses, (b) GIFTS water vapor retrievals with no introduced noise, (c) GIFTS water vapor retrievals with “expected” noise, and (d) GIFTS water vapor retrievals with amplified noise.

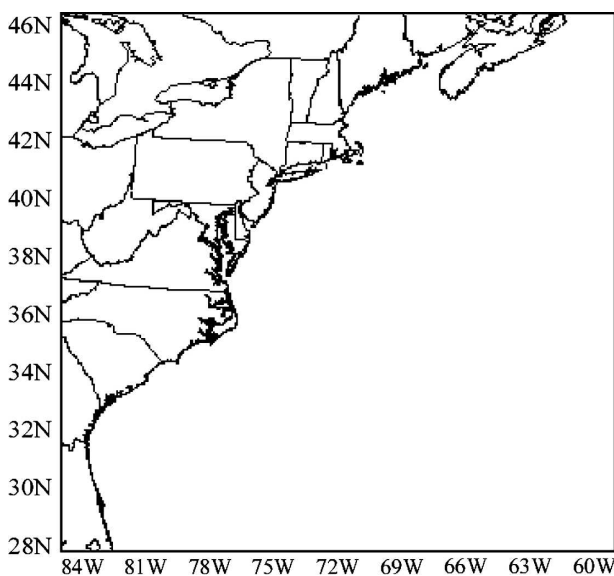


FIG. 9. Geographical domain covered by the WRF simulation.

physics scheme (Hong et al. 2004; Hong and Lim 2006), the Yonsei University PBL scheme, the RRTM long-wave and Dudhia shortwave radiation schemes, and the Noah LSM. No cumulus parameterization scheme was used; therefore, only explicitly resolved convection occurred during the simulation.

The main goal of this case study was to realistically simulate the evolution of the extratropical cyclone and its associated temperature, moisture, and cloud fields. The primary focus of the following analysis is to evaluate the model output during the 6-h period from 1200 until 1800 UTC 5 December 2003. At 1200 UTC, the surface cyclone was located within a strong baroclinic zone along the North Carolina coast (Fig. 10a). A tight pressure gradient and resultant strong winds ahead of the cyclone produced a broad region of warm-air advection over the western Atlantic (not shown). The surface cyclone was located slightly downstream of a weak upper-level shortwave trough that had rotated around the base of a large-scale trough over the Great Lakes

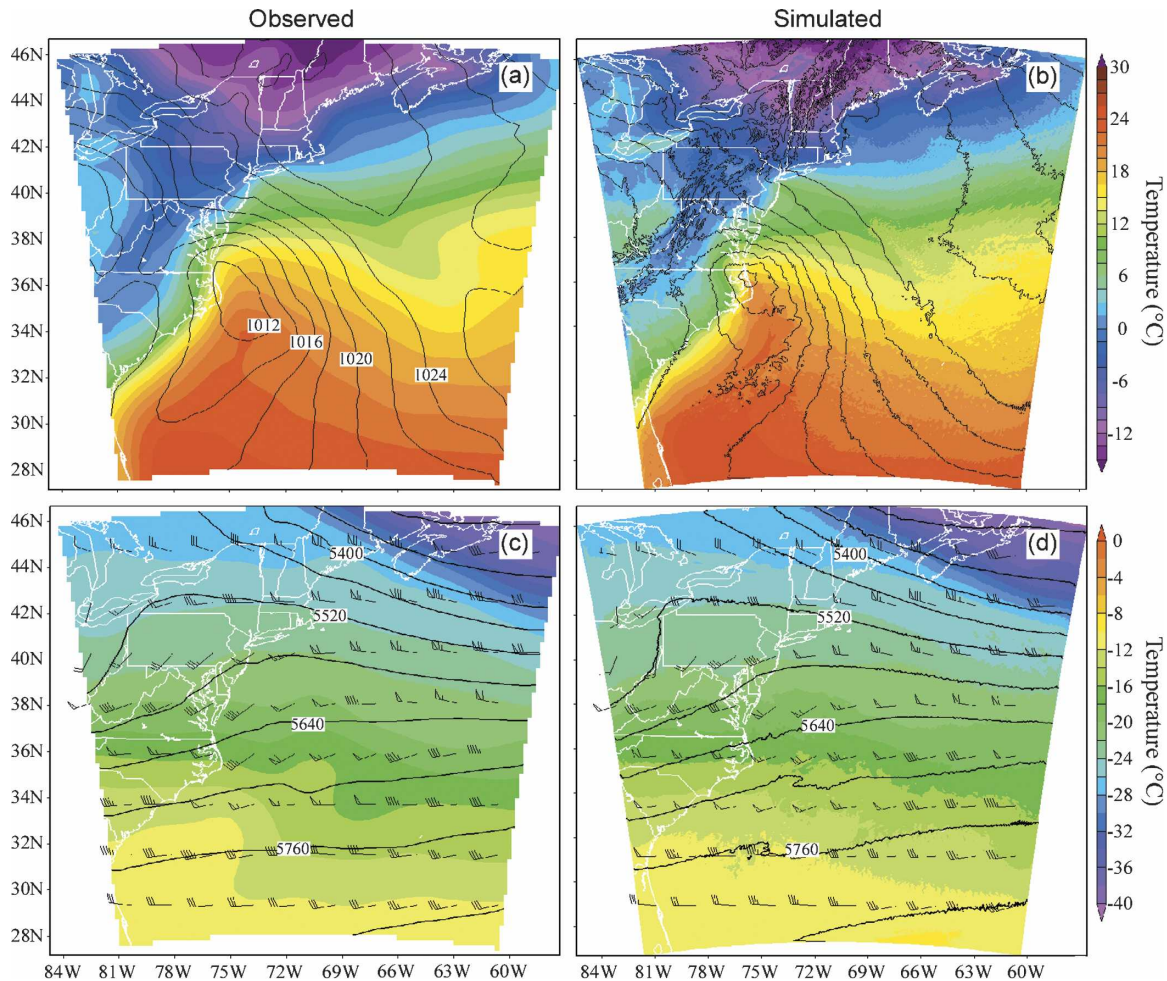


FIG. 10. (a) GFS analyses and (b) WRF-simulated analyses of sea level pressure (hPa; solid line) and 2-m temperature ($^{\circ}\text{C}$; shaded) valid at 1200 UTC 5 Dec 2003. Sea level pressure is contoured every 2 hPa and labeled every 4 hPa. (c) GFS analyses and (d) WRF-simulated analyses of 500-hPa temperature ($^{\circ}\text{C}$; shaded) and geopotential height (m; solid line) valid at 1200 UTC 5 Dec 2003. Geopotential height is contoured every 60 m and labeled every 120 m.

region (Fig. 10c). Comparison with the simulated data (Figs. 10b,d) indicates that the location and magnitude of each of these features are reasonably well depicted by the WRF simulation.

By 1800 UTC, the large-scale upper-level trough had propagated into the western portion of the domain, which resulted in a tighter height gradient over this region and enhanced diffluent flow over the surface cyclone (Figs. 11c,d). In response to the upper-level forcing, the surface cyclone propagated northward along the baroclinic zone and deepened slightly (Figs. 11a,b). A noteworthy feature of the simulated surface data is the presence of a very sharp temperature gradient along the peak of the thermal ridge downstream of the surface cyclone. This feature demonstrates the ability of the WRF model to generate realistic mesoscale thermal structures commonly observed in frontal regions.

GOES-12 satellite imagery and WRF-simulated composite reflectivity (CREF) and vertically integrated cloud microphysics (ICMP) data are shown in Fig. 12. CREF represents the maximum radar reflectivity within a given column, which was calculated using a Rayleigh approximation and the available microphysical data. ICMP represents the total cloud water, rainwater, ice, snow, and graupel content within a given grid column. Together, these data will be used to examine the realism of the simulated cloud field. The visible and infrared satellite images in Fig. 12 illustrate that cloudy conditions were present across much of the domain. The primary cloud features associated with the extratropical cyclone include the extensive mid- and upper-level cloud shield extending from the Atlantic Ocean westward into the Great Lakes region, the low cloud cover over the southeastern United States, and the scattered thunderstorm activity along the trailing

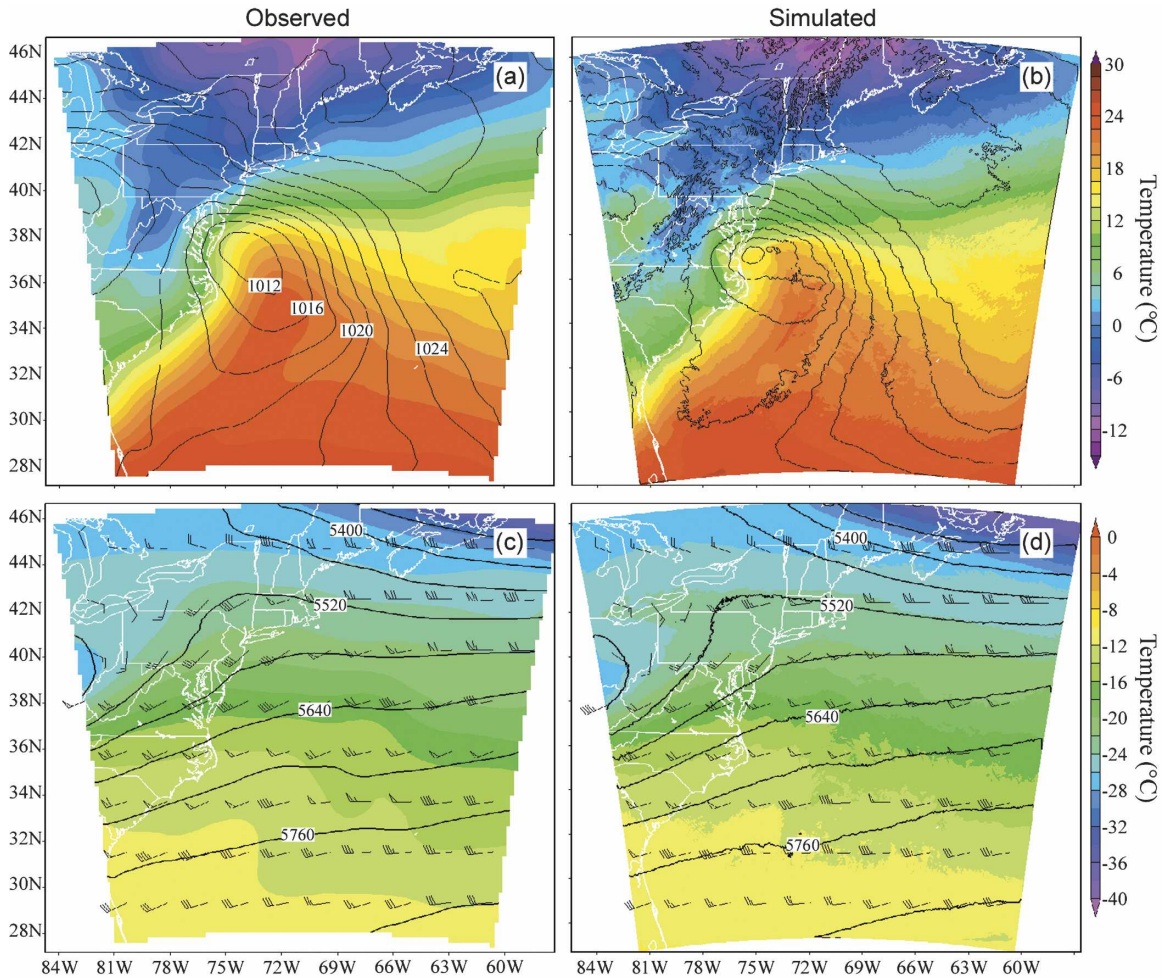


FIG. 11. Same as Fig. 10, except valid at 1800 UTC 5 Dec 2003.

cold front. The CREF and ICMP data indicate that the WRF simulation contains a realistic representation of these features. For instance, the maximum CREF and ICMP values occurred within the region of deep convection along the cold front. Further north, lesser values occurred within the extensive cloud shield, which is consistent with the predominantly stratiform cloud cover across this region. It is also important to note the very finescale structure evident in the simulated cloud fields. Taken together, this analysis demonstrates that the WRF model is able to realistically simulate the finescale atmospheric structures associated with the extratropical cyclone.

A simulated atmospheric profile dataset was generated for this case using the procedure outlined in section 2. This dataset was subsequently ingested into the GIFTS forward model to generate simulated TOA radiances, which were then used to produce simulated temperature and water vapor retrievals. As mentioned

previously, retrievals based on infrared radiances can be calculated down to the earth's surface during clear-sky conditions and above the cloud top during cloudy-sky conditions. The ability to perform retrievals above the cloud top is very important because clouds cover much of the earth's surface at any given moment. The substantial impact that above-cloud retrievals can have on the geographical coverage of the retrieved fields is clearly illustrated in Fig. 13. In the lower troposphere (Figs. 13a,b), the widespread cloud cover associated with the extratropical cyclone severely limits the sampling area of the GIFTS retrievals. Although the retrievals capture a portion of the moisture field surrounding the cyclone, a large portion of the water vapor field is simply not observed. The geographical coverage improves slightly in the midtroposphere (Fig. 13d); however, the cyclone's extensive upper-level cloud shield limits the improvement. The main advantage to performing retrievals above the cloud top becomes ap-

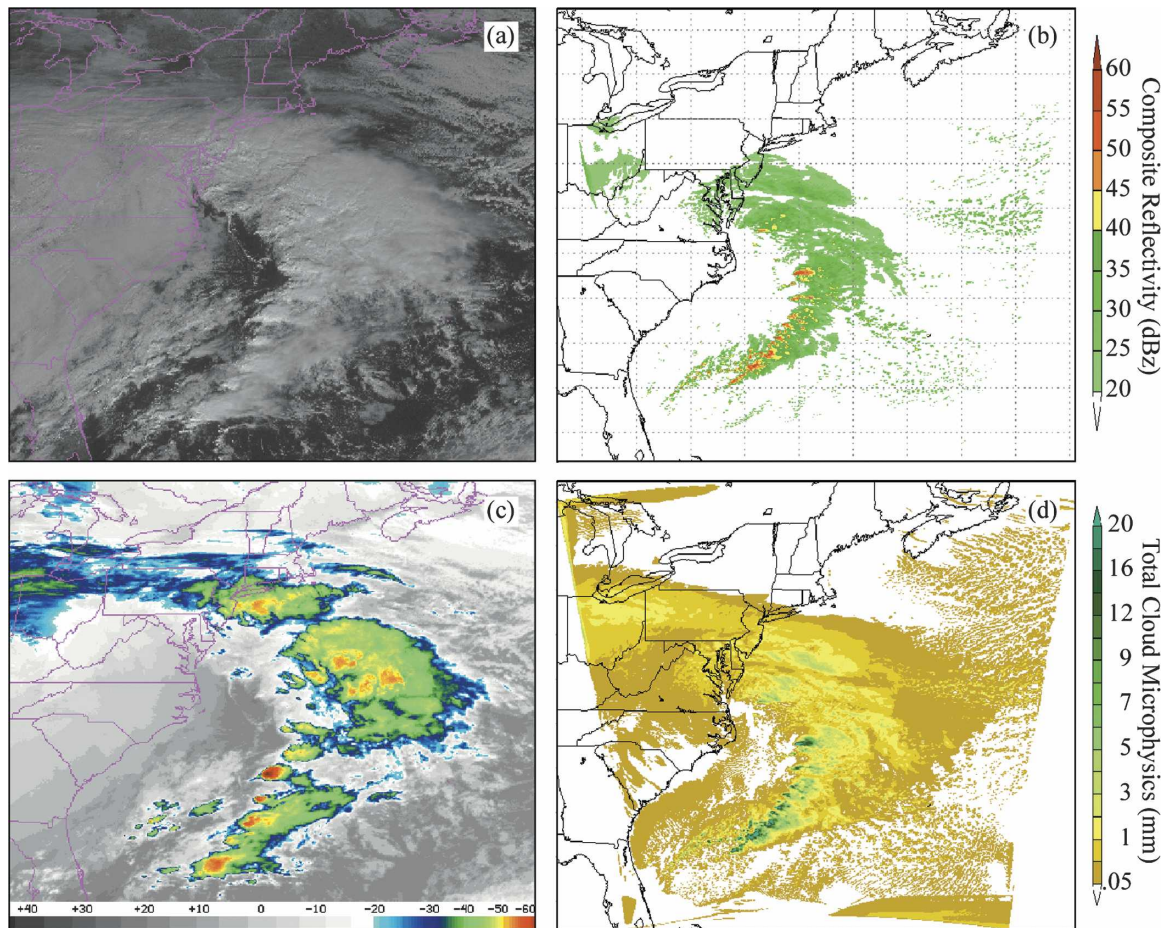


FIG. 12. (a) *GOES-12* visible imagery, (b) WRF-simulated composite reflectivity (dBZ), (c) *GOES-12* 10.7- μm infrared brightness temperatures (K), and (d) WRF-simulated vertically integrated cloud microphysics (mm; cloud water, rainwater, ice, snow, and graupel) valid at 1500 UTC 5 Dec 2003.

parent at 200 hPa (Fig. 13f), where the domain coverage is nearly complete because all but the highest cloud tops occur below this level. The improved coverage at higher altitudes demonstrates that above-cloud retrievals greatly enhance the usefulness of retrievals based on infrared radiances.

4. Conclusions

In this paper, we presented a novel application of NWP models within an end-to-end processing system used to demonstrate advanced hyperspectral satellite technologies and instrument concepts and capabilities. As part of this system, sophisticated NWP models, such as the MM5 and WRF, are used to generate simulated atmospheric profile datasets with fine horizontal and vertical resolution. The primary objective of the numerical modeling work is to produce physically realistic and thermodynamically consistent proxy datasets con-

taining mesoscale cloud, temperature, and water vapor structures representative of the real atmosphere. The simulated proxy datasets, which are treated as the “truth” atmosphere, are subsequently passed through the GIFTS forward radiative transfer model to generate simulated TOA radiances within the GIFTS spectral range. Atmospheric motion vectors and temperature and water vapor retrievals generated from the TOA radiances are then compared with the original model-simulated atmosphere to demonstrate potential hyperspectral measurement capabilities and the potential utility of future wind and retrieval algorithms. Representative examples of TOA radiances, atmospheric motion vectors, and temperature and water vapor retrievals are shown to illustrate the use of the simulated datasets within the end-to-end processing system. Case study results demonstrate that the MM5 and WRF models are both able to realistically simulate mesoscale structures present in the real atmosphere. Because real

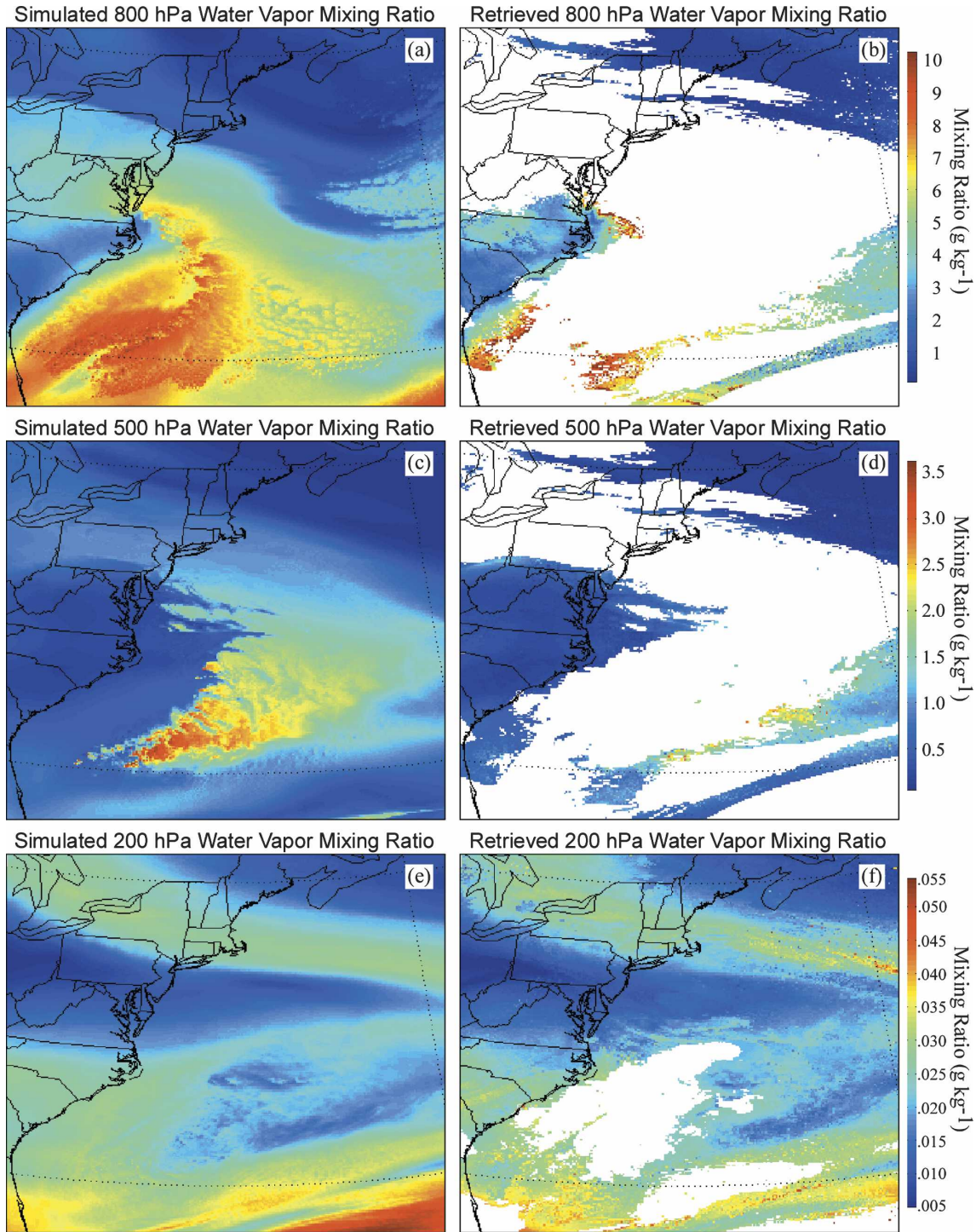


FIG. 13. (a) 800-, (c) 500-, and (e) 200-hPa water vapor mixing ratio (g kg^{-1}) from the WRF simulation, and (b) 800-, (d) 500-, and (f) 200-hPa water vapor mixing ratio (g kg^{-1}) from the simulated GIFTS retrievals valid at 1500 UTC 5 Dec 2003.

hyperspectral radiance measurements with high spatial and temporal resolution are not available for large geographical domains, the simulated TOA radiances represent the only viable alternative to generate proxy

datasets that can be used to demonstrate new hyperspectral technologies. Although the modeling infrastructure described in this paper was specifically tailored to the GIFTS satellite, it should be noted that the

general structure of the forward model allows the end-to-end process to be easily adapted to other infrared sensors, such as ABI and HES.

Future plans include employing a double-moment microphysics scheme that explicitly calculates the mixing ratio and total number concentration of each microphysics species. The inclusion of prognostic number concentrations results in a more realistic simulation of cloud microphysical processes (Morrison et al. 2005; Milbrandt and Yau 2005; Seifert and Beheng 2005; Reisner et al. 1998) and also improves the diagnostic calculation of effective particle diameter used by the forward model. The efficient and accurate infrared cloudy forward model currently under development at CIMSS is a prerequisite for the future assimilation of cloudy infrared radiances in NWP models. Data assimilation studies using the WRF model and infrared radiances generated by the forward model are being planned in order to assess the potential impact that hyperspectral infrared radiances will have on the performance of NWP models. Finally, the NWP modeling infrastructure described in this paper has recently been employed as part of the NOAA GOES-R Risk Reduction (GOES-R3) and Algorithm Working Group (AWG) projects currently underway at CIMSS. A massive model simulation containing a 1580×1830 grid-point domain covering most of North and South America with 8-km horizontal grid spacing was used to produce a simulated atmospheric profile dataset for these projects. Additional simulations employing very fine horizontal grid spacing (<1 km) over smaller geographical domains will also be used to demonstrate the advanced high-spatial-resolution imaging and high-spectral-resolution sounding synergistic sensing capability of future satellites.

Acknowledgments. This work was sponsored by the Office of Naval Research under MURI Grant N00015-01-1-0850 and by the National Oceanic and Atmospheric Administration under GOES-R Grant NA07EC0676. The detailed suggestions of three anonymous reviewers enhanced the presentation of the manuscript.

REFERENCES

- Chen, F., and J. Dudhia, 2001: Coupling an advanced land surface-hydrology model with the Penn State-NCAR MM5 modeling system. Part I: Model implementation and sensitivity. *Mon. Wea. Rev.*, **129**, 569–585.
- Clough, S. A., and M. J. Iacono, 1995: Line-by-line calculations of atmospheric fluxes and cooling rates. 2: Applications to carbon dioxide, ozone, methane, nitrous oxide and the halocarbons. *J. Geophys. Res.*, **100**, 16 519–16 535.
- Davies, J. E., E. R. Olson, and D. J. Posselt, 2003: Cloud model upgrade to the GIFTS Fast Radiative Transfer Model. University of Wisconsin—Madison, Space Science and Engineering Center, UW-SSEC Publication 03.09.D1, 44 pp.
- Dudhia, J., 1989: Numerical study of convection observed during the Winter Monsoon Experiment using a mesoscale two-dimensional model. *J. Atmos. Sci.*, **46**, 3077–3107.
- , D. Gill, K. Manning, W. Wang, C. Bruyere, J. Wilson, and S. Kelly, 2003: PSU/NCAR mesoscale modeling system tutorial class notes and users guide. MM5 Modeling System version 3, Mesoscale and Microscale Meteorology Division, National Center for Atmospheric Research, 390 pp.
- Grasso, L. D., 2000: The differentiation between grid spacing and resolution and their application to numerical modeling. *Bull. Amer. Meteor. Soc.*, **81**, 579–580.
- Grell, G. A., J. Dudhia, and D. R. Stauffer, 1994: A description of the Fifth-Generation Penn State/NCAR Mesoscale Model (MM5). NCAR Tech. Note NCAR/TN 398+STR, 117 pp.
- Hong, S.-Y., and H.-L. Pan, 1996: Nonlocal boundary layer vertical diffusion in a medium-range forecast model. *Mon. Wea. Rev.*, **124**, 2322–2339.
- , and J.-O. Lim, 2006: The WRF single-moment 6-class microphysics scheme (WSM6). *J. Korean Meteor. Soc.*, **42**, 129–151.
- , J. Dudhia, and S.-H. Chen, 2004: A revised approach to ice microphysical processes for the bulk parameterization of clouds and precipitation. *Mon. Wea. Rev.*, **132**, 103–120.
- Li, J., and H.-L. Huang, 1999: Retrieval of atmospheric profiles from satellite sounder measurements by use of the discrepancy principle. *Appl. Opt.*, **38**, 916–923.
- , W. Wolf, W. P. Menzel, W. Zhang, H.-L. Huang, and T. H. Achter, 2000: Global soundings of the atmosphere from ATOVS measurements: The algorithm and validation. *J. Appl. Meteor.*, **39**, 1248–1268.
- , F. Sun, S. Seemann, E. Weisz, and H.-L. Huang, 2004: GIFTS sounding retrieval algorithm development. Preprints, *20th Int. Conf. on Interactive Information and Processing Systems (IIPS) for Meteorology, Oceanography, and Hydrology*, Seattle, WA, Amer. Meteor. Soc., CD-ROM, P2.32.
- Lin, L.-H., R. D. Farley, and H. D. Orville, 1983: Bulk parameterization of the snow field in a cloud model. *J. Climate Appl. Meteor.*, **22**, 1065–1092.
- Milbrandt, J. A., and M. K. Yau, 2005: A multimoment bulk microphysics parameterization. Part I: Analysis of the role of the spectral shape parameter. *J. Atmos. Sci.*, **62**, 3051–3064.
- Mitchell, D. L., 2002: Effective diameter in radiative transfer: General definition, applications, and limitations. *J. Atmos. Sci.*, **59**, 2330–2346.
- Mlawer, E. J., S. J. Taubman, P. D. Brown, and M. J. Iacono, 1997: Radiative transfer for inhomogeneous atmospheres: RRTM, a validated correlated-k model for the longwave. *J. Geophys. Res.*, **102**, 16 663–16 682.
- Morrison, H., J. A. Curry, M. D. Shupe, and P. Zuidema, 2005: A new double-moment microphysics parameterization for application in cloud and climate models. Part II: Single-column modeling of arctic clouds. *J. Atmos. Sci.*, **62**, 1678–1693.
- Moy, L., D. Tobin, P. van Delst, and H. Woolf, 2004: Clear sky forward model development for GIFTS. Preprints, *20th Int. Conf. on Interactive Information and Processing Systems (IIPS) for Meteorology, Oceanography, and Hydrology*, Seattle, WA, Amer. Meteor. Soc., CD-ROM, P.2.35.
- Nieman, S., J. Schmetz, and W. P. Menzel, 1993: A comparison of several techniques to assign heights to cloud tracers. *J. Appl. Meteor.*, **32**, 1559–1568.

- Niu, J., P. Yang, H.-L. Huang, J. E. Davies, J. Li, B. A. Baum and Y. X. Hu, 2007: A fast infrared radiative transfer model for overlapping clouds. *J. Quant. Spectrosc. Radiat. Transfer*, **103**, 447–459.
- Pielke, R. A., 2002: *Mesoscale Meteorological Modeling*. 2d ed. Academic Press, 676 pp.
- Reisner, J., R. Bruintjes, and R. Rasmussen, 1998: An examination on the utility of forecasting supercooled liquid water in a mesoscale model. *Quart. J. Roy. Meteor. Soc.*, **124**, 1071–1107.
- Schmit, T. J., J. Li, and J. Gurka, 2003: Introduction of the Hyperspectral Environmental Suite (HES) on GOES-R and beyond. *Proc. 13th Int. TOVS Study Conf.*, Ste-Adele, QC, Canada, University of Wisconsin, 577–584.
- , M. M. Gunshor, W. P. Menzel, J. J. Gurka, J. Li, and A. S. Bachmeier, 2005: Introducing the next-generation Advanced Baseline Imager on GOES-R. *Bull. Amer. Meteor. Soc.*, **86**, 1079–1096.
- Seifert, A., and K. D. Beheng, 2005: A two-moment cloud microphysics parameterization for mixed-phase clouds. Part 1: Model description. *Meteor. Atmos. Phys.*, **92**, 45–66.
- Skamarock, W. C., 2004: Evaluating mesoscale NWP models using kinetic energy spectra. *Mon. Wea. Rev.*, **132**, 3019–3032.
- , J. B. Klemp, J. Dudhia, D. O. Gill, D. M. Barker, W. Wang, and J. G. Powers, 2005: A description of the Advanced Research WRF version 2. NCAR Tech. Note NCAR/TN-468+STR, 88 pp.
- Smith, W. L., and Coauthors, 2001: The Geosynchronous Imaging Fourier Transform Spectrometer (GIFTS). Preprints, *11th Conf. on Satellite Meteorology and Oceanography*, Madison, WI, Amer. Meteor. Soc., 700–707.
- , and Coauthors, 2003: Validation of satellite AIRS retrievals with aircraft NAST-I soundings and dropsondes: Implications for future satellite sounding capabilities. *Proc. 13th Int. TOVS Study Conf.*, Ste-Adele, QC, Canada, University of Wisconsin, 382–394.
- , D. K. Zhou, H.-L. Huang, J. Li, X. Liu, and A. M. Larar, 2004: Extraction of profile information from cloud contaminated radiances. *Proc. ECMWF Workshop on the Assimilation of High Spectral Resolution Sounders in NWP*, Reading, United Kingdom, ECMWF, 145–154.
- Stamnes, K., S. C. Tsay, W. Wiscombe, and K. Jayaweera, 1988: A numerically stable algorithm for discrete-ordinate-method radiative transfer in multiple scattering and emitting layered media. *Appl. Opt.*, **27**, 2502–2509.
- Stauffer, D. R., and N. L. Seaman, 1990: Use of four-dimensional data assimilation in a limited-area mesoscale model. Part I: Experiments with synoptic-scale data. *Mon. Wea. Rev.*, **118**, 1250–1277.
- Tao, W.-K., and J. Simpson, 1993a: Goddard Cumulus Ensemble Model. Part I: Model description. *Terr. Atmos. Oceanic Sci.*, **4**, 35–72.
- , and —, 1993b: Goddard Cumulus Ensemble Model. Part II: Applications for studying cloud precipitating processes and for NASA TRMM. *Terr. Atmos. Oceanic Sci.*, **4**, 73–116.
- Tobin, D., and Coauthors, 2001: Simulation of GIFTS data cubes. Preprints, *11th Conf. on Satellite Meteorology and Oceanography*, Madison, WI, Amer. Meteor. Soc., 563–565.
- Velden, C., C. Hayden, S. Nieman, W. P. Menzel, S. Wanzong, and J. S. Goerss, 1997: Upper-tropospheric winds derived from geostationary satellite water vapor observations. *Bull. Amer. Meteor. Soc.*, **78**, 173–195.
- , and Coauthors, 2005: Recent innovations in deriving tropospheric winds from meteorological satellites. *Bull. Amer. Meteor. Soc.*, **86**, 205–223.
- Wei, H., P. Yang, J. Li, B. A. Baum, H.-L. Huang, S. Platnick, Y. Hu, and L. Strow, 2004: Retrieval of semitransparent ice cloud optical thickness from Atmospheric Infrared Sounder (AIRS) measurements. *IEEE Trans. Geosci. Remote Sens.*, **42**, 2254–2267.
- Weisz, E., H.-L. Huang, J. Li, S. Wetzel-Seemann, E. Borbas, and L. Gumley, 2003: AIRS real-time sounding profile retrieval for IMAPP users. *Proc. 13th Int. TOVS Study Conf.*, Ste-Adele, QC, Canada, University of Wisconsin, 323–330.
- Yang, P., H.-L. Wei, B. A. Baum, H.-L. Huang, A. J. Heymsfield, Y. X. Hu, B.-C. Gao, and D. D. Turner, 2003: The spectral signature of mixed-phase clouds composed of non-spherical ice crystals and spherical liquid droplets in the terrestrial window region. *J. Quant. Spectrosc. Radiat. Transfer*, **79–80**, 1171–1188.